Laser patterning and electrochemical characterization of thick-film cathodes for lithium-Ion batteries

Penghui Zhu, Peter Smyrek, Benjamin Ebert, Wilhelm Pfleging
Karlsruhe Institute of Technology (KIT), IAM-AWP, Hermann-von-Helmholtz-Platz 1, 76344 Eggenstein-Leopoldshafen, Germany

ABSTRACT

Lithium-ion batteries (LIBs) are currently dominating the electrochemical storage sector due to their excellent properties such as high energy density, high power density, and long cycle lifetime. For automotive applications, current research focuses on the merger of two concepts: (i) the "thick film concept" which enables a high energy density due to a reduced amount of inactive materials, and (ii) the "three-dimensional (3D) battery concept", which provides a high power density with improved interfacial kinetics at mass loadings $\geqslant$ 35 mg/cm^2. Latter could be realized by applying ultrafast laser patterning of electrodes, which in turn includes an advanced 3D electrode design. Briefly, a rapid and homogeneous electrode wetting with liquid electrolyte can be induced, and besides a high capacity retention during long-term cyclability. Recently, various electrode designs such as line, grid, and hole structures have been reported for cathodes and anodes. However, the mass loss of those electrodes needs to be considered, since the cathode represents about 50 % of the total material costs of LIBs. Thus, the use of electrode structures with a high aspect ratio as well as a significantly reduced material removal is of great importance. In this work, 150 µm thick-film $Li(Ni_{0.6}Mn_{0.2}Co_{0.2})O_2$ electrodes were manufactured by roll-to-roll tape-casting and subsequently structured with different pattern types using ultrafast laser radiation. Additionally, different designs were applied for laser patterning and the mass loss was minimized down to 7 %. Finally, the cathodes were assembled in half-cells for studying the impact of different laser patterning designs on electrochemical performance.

Keywords: ultrafast laser patterning; lithium-ion battery; thick-film cathode; NMC 622

1. INTRODUCTION

Lithium-ion batteries (LIBs) are dominating the electrochemical storage sectors such as portable devices, stationary grid storage, and electric power tools[1]. The success of LIBs lies in their superior properties such as high energy density and high power in comparison to as Ni-Cd or Na-ion batteries[2]. Nowadays, with the rapid development of battery electric vehicles (BEV), the demand for batteries with high capacity, fast charging, high power, long lifetime, low cost, and safety under different conditions, is becoming more significant for the automobile industries[3, 4]. In order to achieve a higher energy density, it is practical to choose cathode materials with high specific capacities. Layered lithium transition metal oxide $Li(Ni_xMn_yCo_{1-x-y})O_2$ (NMC) is a popular candidate for BEVs due to its high energy density in comparison to other cathode materials such as $LiCoO_2$ (LCO), $LiFePO_4$ (LFP), and $LiMn_2O_4$ (LMO)[5, 6].

Increasing the film thickness or mass loading is a practical strategy to increase the energy density of LIBs, since less inactive materials are needed during cell assembly, which also leads to cost reduction in battery manufacturing[7]. However, the power density decreases rapidly with increasing film thickness[8]. This is mainly due to an increasing cell polarization, local materials degradation, as well as lithium-ion diffusion limitation, which leads to an increase in charge transfer resistance[9]. Battery with 3D architectures generated by ultrafast laser patterning is beneficial to increase energy density and power density simultaneously, since the lithium-ion diffusion kinetics in thick-film electrodes is improved[10–12]. Meanwhile, an accelerated electrolyte wetting in laser patterned electrodes due to the capillary microstructures is observed[13]. Our previous works displayed that the cells with laser patterned NMC electrodes exhibit high capacity retention after long-term cycling and show higher capacity at fast charge and discharge rates over C/2 in comparison to reference cells with unstructured electrodes.[8, 14, 15], while other researchers observed similar phenomenon using other cathode materials such as LCO with line structures[16], and LFP with hole structures[17]. Besides, laser patterned graphite-based anodes (with or without silicon) with lines, grids, and holes display high capability at elevated C-rates [18–21]. Hence, laser patterning is a powerful method to improve battery performance, especially in combination with thick-film electrodes.

In this work, we present the study of polyvinylidene fluoride (PVDF)-based thick-film $Li(Ni_{0.6}Mn_{0.2}Co_{0.2})O_2$ (NMC 622) electrodes using different 3D designs by applying ultrafast laser patterning. The mass loss due to laser ablation is kept under 10 % for different designs. The electrochemical performance of cells containing cathodes with different patterns is analyzed using rate capability and lifetime analysis.

2. EXPERIMENTAL

2.1 Preparation of thick-film NMC cathodes

Commercially available NMC 622 powder (BASF SE, Germany) with a median particle size of 8.7 µm was used as active material, while C-NERGY Super C65 (Imerys G & C, Belgium) and C-NERGY KS6L graphite (Imerys G & C, Switzerland) were applied as conductive additive and compaction aid, respectively. 24 hours prior to slurry preparation, Solef 5130 PVDF binder (Solvay, Germany) was dissolved in N-methyl-2-pyrrolidone (NMP, Merck, Germany) with 1:10 mass ratio using a laboratory dissolver DB 13 (DISTECH, Germany) equipped with a vacuum pump. Subsequently, other components were added into PVDF solution with NMC 622: Super C65: KS6L graphite: PVDF (powder) = 92: 3: 2: 3 (wt.%). The slurry was mixed using the same dissolver for 1.5 h with 500-2000 rpm, while extra NMP solution was added into the mixture to adjust the slurry viscosity. The mixing process was conducted at room temperature.

NMP-based slurry was then deposited onto an aluminum-foil (thickness: 15 µm) applying a doctor blade ZUA 2000.100 (Proceq, Switzerland) and a modified roll-to-roll coater TMAX-JCT-150 (Xiamen Tmax Battery Equipments, China). The coating speed was set at 5.6 mm/s and the electrodes were dried at 100 °C in a chamber of 1.2 m length. The thicknesses of dried electrodes were kept about 185 µm to achieve thick-film electrodes with a mass loading of 40 mg/cm^2. Finally, dried cathodes were calendered using an electric rolling presser MSK-2150 (MTI Corporation, USA) with a constant calendering speed of 35 mm/s to adjust the electrode porosity to 35 %. The electrode porosity was calculated based on the density and weight of each component[8].

2.2 Ultrafast laser ablation of NMC cathodes

Ultrafast femtosecond (fs) laser FX600 (Edgewave, Germany) with 600 fs pulse duration and a wavelength of 1030 nm ($M^2 < 1.1$) was applied as laser source, while an IntelliSCAN III 20 scanner (Scanlab, Germany) equipped with an F-theta lens F255 (Scanlab, Germany) were used for the laser patterning of NMC 622 cathodes. Four different designs were applied, which are lines (Li), holes (Ho), lines and holes (LiHo), and hexagonal (Hex) structures. The repetition rate, laser power, and scan speed for laser patterning of NMC 622 electrodes with different designs are listed in Table 1. Scan passes were adjusted to achieve line or hole structured from electrode surface down to the current collector, without damaging the current collector. The mass loss due to laser ablation was adjusted to around 7 %. The laser patterning was performed in ambient air with an extraction device on the side. After laser ablation, the electrodes were cut in circles with 12 mm in diameter for coin cell CR2032 design.

Table 1. Laser parameters for patterning of NMC 622 electrodes with different designs.

Designs	Laser power (W)	Repetition rate (kHz)	Scan speed (m/s)
Lines (Li)	46	1500	20
Holes (Ho)	86	100	10
Lines+holes (LiHo)	73	1500	10
Hexagonal (Hex)	35	1500	5

2.3 Cell assembly and electrochemical analysis

NMC 622 cathodes were dried at 130 °C for 24 h in a vacuum oven (VT 6025, Thermo Scientific, Germany) before cell assembly. Afterwards, the cathodes were assembled versus lithium foil with 0.25 mm thickness (Merck, Germany) in coin cells CR2032 in an argon-filled glove box LABmaster pro (M. Braun, Germany) with $H_2O < 0.1$ ppm and $O_2 < 0.1$ ppm. Polypropylene (PP) separator foil (Celgard, USA) with a thickness of 25 µm was placed between NMC 622 electrode and lithium. A total amount of 120 µL electrolyte, which consists of ethylene carbonate and ethyl methyl carbonate (EC/EMC 3:7, wt.%) with 1.3 M hexafluorophosphate ($LiPF_6$) as conducting salt and 5 wt.% fluoroethylene carbonate (FEC) as

additive, was added to each cell. All cell components were pressed and sealed with an electric crimper MSK-160D (MTI Corporation, USA).

For rate capability analysis, "constant current-constant voltage" (CCCV) method was applied using a battery cycling system BT 2000 (Arbin Instruments, USA). After cell assembly, 3 cycles at C/20 were applied as formation step, followed by increasing C-rates from C/10 to 1C. C/10 and C/5 were performed for 5 cycles, while 10 cycles were carried out at C/2 and 1C. For C/2 and 1C, the charge rates were kept constant at C/2, while the same charge and discharge rates are used from C/20 to C/5. A specific capacity of 172 mAh/g and 1C = 0.99 h^{-1} were applied to calculate the charge/discharge current at different C-rates. For rate capability analysis, the voltage window was set to 3.0–4.3 V.

3. RESULTS AND DISCUSSION

3.1 Characterization of laser patterned electrodes

The drying chamber has a length of 1.2 m, while a band speed of 5.6 mm/s was applied, thus the NMP solvent in electrode after casting must be dried within 3.6 min to realize a continuous roll-to-roll coating process. Due to a limited drying rate, the realization of thick film electrodes was established via a multilayer concept. The film thickness after calendering is 154 µm. The respective active mass loading and areal capacity are 38 mg/cm^2 and 6.5 mAh/cm^2, respectively.

The schematics of laser patterned NMC 622 electrodes with four different designs are shown in Figure 1. For line structures, a pitch of 200 µm was applied (Figure 1-a), while Figure 1-b exhibit LiHo structures, which have a pitch of 450 µm between lines and 130 µm distance between holes. In Figure 1-c, holes arranged in equilateral triangles with 130 µm length were processed with constant scanning speed (10 m/s). The diameter of holes at the electrode surface is 50 µm. In order to achieve hexagonal structures, the scan speed was adjusted to 5 m/s and the laser power was decreased. Each side of the hexagon has a length of 300 µm, as depicted in Figure 1-d. Besides, no melted particles or obvious heat affected zones could be detected.

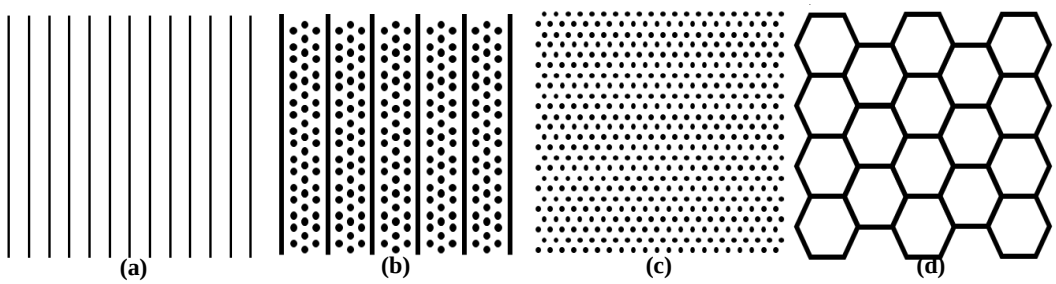

Figure 1. Schematics of laser patterned NMC 622 electrodes with (a) lines structures, (b) LiHO structures, (c) holes, and (d) hexagonal structures.

By adjusting the pitch and arrangement in different designs, the mass loss is kept ~ 7 % for electrodes with different designs, as listed in Table 2.

Table 2. Mass loss, and areal capacity of laser patterned NMC 622 cathodes with different designs.

Electrode design	Mass loss (%)	Areal capacity (mAh/cm^2)	Active mass loading (mg/cm^2)
Unstructured	-	6.5	37.6
Li	6.1	6.1	35.3
LiHo	6.7	6.1	35.1
Ho	7.4	6.0	34.8
Hex	6.5	6.1	35.2

3.2 Electrochemical performance of cells

Rate capability analysis and lifetime analysis were performed to study the effect of different laser patterning designs on the electrochemical performance of cells. Figure 2 shows the specific discharge capacities of cells with different types of electrodes with increasing C/rates from C/20 to 1C. During formation step, cells with unstructured electrodes show 173 mAh/g discharge capacity, while cells containing electrodes with hexagonal structures exhibit 169 mAh/g capacity. A decrease in discharge capacity at low C-rates is most likely due to the side reactions between electrolyte and NMC 622 particles on the electrode surface during formation, this is also reported in our previous works[8, 15]. At C/10, no difference in specific capacity is observed between cells with different patterned electrodes. At C/5, cells containing electrodes with Li and LiHo structures show 5 mAh/g higher capacity in comparison to ones with Hex and Ho structures as well as reference cells with unstructured electrodes. The advantages of laser patterning is more obvious at C/2 and 1C. For example, at C/2 all cells with laser patterned electrodes provide ~150 mAh/g capacity, while the capacity of reference cells drop to 120 mAh/g. The difference is more profound at 1C between reference cells and cells with patterned electrodes. All cells with laser patterned electrodes display 120-125 mAh/g capacities, while reference cells show about 50 mAh/g capacity, which means that a capacity increase of around 130 % is achieved by introducing laser patterning into the electrode processing.

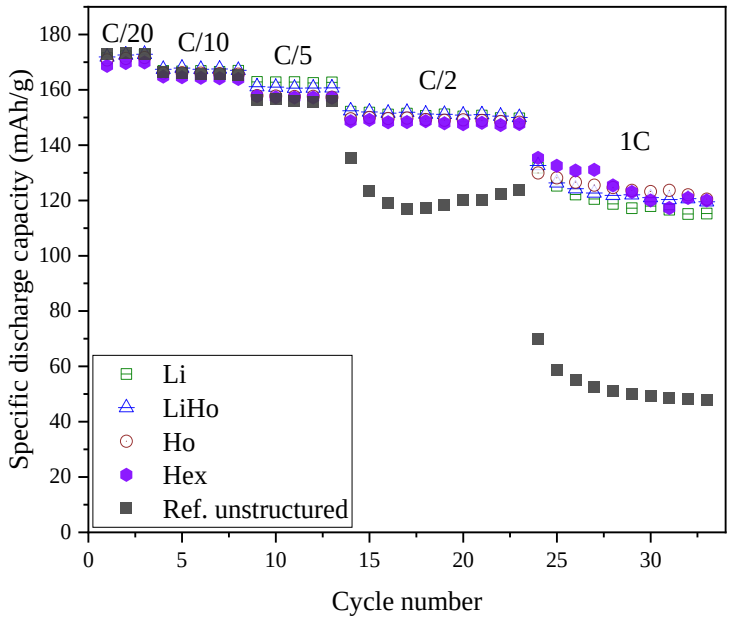

Figure 2. Rate capability analysis of cells containing laser patterned NMC 622 cathodes with different electrode designs.

The average discharge capacities at C/20, C/5, and 1C as well as capacity increase at 1C of cells with different types of NMC 622 electrodes are summarized in Table 3. From rate capability analysis it is hard to conclude which design is the optimal, since all cells with laser patterned electrodes show similar capacity increase at high C-rates. However, considering the processing time and complexity of laser patterning, line structures are preferable, since it is more practical for upscaling in industrial applications.

Table 3. The average discharge capacity at C/20, C/5 and 1C, as well as capacity increase at 1C of cells with different types of laser patterned electrodes in comparison to reference cells.

Electrode designs	Average discharge capacity at C/20 (mAh/g)	Average discharge capacity at C/5 (mAh/g)	Average discharge capacity at 1C (mAh/g)	Capacity increase at 1C (%)
unstructured	173.0	156.1	53.1	-
Li	172.1	162.7	120.1	126
LiHo	172.5	160.8	123.1	132
Ho	171.3	157.6	124.8	135
Hex	169.4	157.3	125.6	137

The high capacity at high C-rates of cells with laser patterned electrodes is mainly due to an improved lithium-ion diffusion kinetics in cells[11]. Smyrek et al.[11] and Park et al.[22] reported that the capacity loss of cells with thick-film electrodes is owing to the accumulated lithium-ion transport limitation and locally increased ohmic resistance. They also verified that the active materials at the bottom layer closed to the current collector participate no longer in the electrochemical reaction and maintain the same state-of-charge (SOC) regardless of the charge or discharge. However, after laser patterning, the new generated contact surfaces between electrolyte and electrode materials can alleviate the locally increased ohmic resistance and new diffusion pathways of lithium-ions are generated from electrolyte to the bulk electrode. Besides, Heubner et al.[23] investigated the relationship between energy and power density and proved that that energy density increases with increasing mass loading and lower porosity, while power density decreases rapidly. With laser patterning, channels or holes are generated, which provide extra porosity in electrodes, while the not patterned parts remain a low porosity and a high mass loading. Thus the power density and energy density can be increased simultaneously.

4. CONCLUSIONS

PVDF-based thick-film NMC 622 cathodes were tape-cast and dried using roll-to-roll process. The electrodes were then patterned with different designs using femtosecond laser ablation. Lines, lines and holes, holes, and hexagonal structured were generated in NMC 622 electrodes and the mass loss was kept constant at ~ 7 %. The laser patterned electrodes were then assembled versus lithium in half cells for electrochemical analysis. Rate capability analysis displays that the cells with laser patterned electrodes show higher discharge capacity in comparison to reference cells, especially at high C-rates such as C/2 and 1C. For example, around 130 % capacity increase was observed at 1C. Lifetime analysis exhibits that the cells with LiHo structures have the highest the initial capacity as well as the highest cycling stability after 50 cycles. After comparing the Li, Ho, and LiHo structures, it is concluded that with the combination of lines and holes structures, the cells show the highest cycling stability and high capability at C-rates > C/5.

5. ACKNOWLEDGMENT

We are grateful to the help of our colleagues A. Reif, H. Besser, and M. Kapitz for their technical support in laser processing and electrode characterization. This research was funded by Federal Ministry of Education and Research (BMBF), project NextGen-3DBat, project No. 03XP01798F.

REFERENCES

[1] Armand, M., Axmann, P., Bresser, D., Copley, M., Edström, K., Ekberg, C., Guyomard, D., Lestriez, B., Novák, P. and Petranikova, M., "Lithium-ion batteries–Current state of the art and anticipated developments," Journal of Power Sources 479, 228708 (2020).

[2] Bashir, T., Ismail, S. A., Song, Y., Irfan, R. M., Yang, S., Zhou, S., Zhao, J. and Gao, L., "A review of the energy storage aspects of chemical elements for lithium-ion based batteries," Energy Materials 1(2), 100019 (2021).

[3] Ding, Y., Cano, Z. P., Yu, A., Lu, J. and Chen, Z., "Automotive Li-ion batteries: current status and future perspectives," Electrochemical Energy Reviews 2(1), 1–28 (2019).

[4] Masias, A., Marcicki, J. and Paxton, W. A., "Opportunities and challenges of lithium ion batteries in automotive applications," ACS energy letters 6(2), 621–630 (2021).
[5] Cano, Z. P., Banham, D., Ye, S., Hintennach, A., Lu, J., Fowler, M. and Chen, Z., "Batteries and fuel cells for emerging electric vehicle markets," Nature Energy 3(4), 279–289 (2018).
[6] Wang, X., Ding, Y.-L., Deng, Y.-P. and Chen, Z., "Ni‐Rich/Co‐poor layered cathode for automotive Li‐ion batteries: promises and challenges," Advanced Energy Materials 10(12), 1903864 (2020).
[7] Wood III, D. L., Li, J. and Daniel, C., "Prospects for reducing the processing cost of lithium ion batteries," Journal of Power Sources 275, 234–242 (2015).
[8] Zhu, P., Seifert, H. J. and Pfleging, W., "The ultrafast laser ablation of $Li(Ni_{0.6}Mn_{0.2}Co_{0.2})O_2$ electrodes with high mass loading," Applied Sciences 9(19), 4067 (2019).
[9] Park, K.-Y., Park, J.-W., Seong, W. M., Yoon, K., Hwang, T.-H., Ko, K.-H., Han, J.-H., Jaedong, Y. and Kang, K., "Understanding capacity fading mechanism of thick electrodes for lithium-ion rechargeable batteries," Journal of Power Sources 468, 228369 (2020).
[10] Pfleging, W., "A review of laser electrode processing for development and manufacturing of lithium-ion batteries," Nanophotonics 7(3), 549–573 (2018).
[11] Smyrek, P., Bergfeldt, T., Seifert, H. J. and Pfleging, W., "Laser-induced breakdown spectroscopy for the quantitative measurement of lithium concentration profiles in structured and unstructured electrodes," Journal of Materials Chemistry A 7(10), 5656–5665 (2019).
[12] Pfleging, W., "Recent progress in laser texturing of battery materials: A review of tuning electrochemical performances, related material development, and prospects for large-scale manufacturing," International Journal of Extreme Manufacturing 3(1), 12002 (2020).
[13] Pfleging, W. and Pröll, J., "A new approach for rapid electrolyte wetting in tape cast electrodes for lithium-ion batteries," Journal of Materials Chemistry A 2(36), 14918–14926 (2014).
[14] Song, Z., Zhu, P., Pfleging, W. and Sun, J., "Electrochemical performance of thick-film $Li(Ni_{0.6}Mn_{0.2}Co_{0.2})O_2$ cathode with hierarchic structures and laser ablation," Nanomaterials 11(11), 2962 (2021).
[15] Zhu, P., Han, J. and Pfleging, W., "Characterization and laser structuring of aqueous processed $Li(Ni_{0.6}Mn_{0.2}Co_{0.2})O_2$ thick-film cathodes for lithium-ion batteries," Nanomaterials 11(7), 1840 (2021).
[16] Park, J., Jeon, C., Kim, W., Bong, S.-J., Jeong, S. and Kim, H.-J., "Challenges, laser processing and electrochemical characteristics on application of ultra-thick electrode for high-energy lithium-ion battery," Journal of Power Sources 482, 228948 (2021).
[17] Tsuda, T., Ishihara, Y., Watanabe, T., Ando, N., Gunji, T., Soma, N., Nakamura, S., Hayashi, N., Ohsaka, T. and Matsumoto, F., "An Improved High-rate Discharging Performance of "Unbalanced" $LiFePO_4$ Cathodes with Different $LiFePO_4$ Loadings by a Grid-patterned Micrometer Size-holed Electrode Structuring," Electrochemistry 87(6), 370–378 (2019).
[18] Zheng, Y., Seifert, H. J., Shi, H., Zhang, Y., Kübel, C. and Pfleging, W., "3D silicon/graphite composite electrodes for high-energy lithium-ion batteries," Electrochimica Acta 317, 502–508 (2019).
[19] Meyer, A., Ball, F. and Pfleging, W., "The Effect of Silicon Grade and Electrode Architecture on the Performance of Advanced Anodes for Next Generation Lithium-Ion Cells," Nanomaterials 11(12), 3448 (2021).
[20] Kriegler, J., Hille, L., Stock, S., Kraft, L., Hagemeister, J., Habedank, J. B., Jossen, A. and Zaeh, M. F., "Enhanced performance and lifetime of lithium-ion batteries by laser structuring of graphite anodes," Applied Energy 303, 117693 (2021).
[21] Dubey, R., Zwahlen, M.-D., Shynkarenko, Y., Yakunin, S., Fuerst, A., Kovalenko, M. V. and Kravchyk, K. V., "Laser Patterning of High‐Mass‐Loading Graphite Anodes for High‐Performance Li‐Ion Batteries," Batteries & Supercaps 4(3), 464–468 (2021).
[22] Park, K.-Y., Park, J.-W., Seong, W. M., Yoon, K., Hwang, T.-H., Ko, K.-H., Han, J.-H., Jaedong, Y. and Kang, K., "Understanding capacity fading mechanism of thick electrodes for lithium-ion rechargeable batteries," Journal of Power Sources 468, 228369 (2020).
[23] Heubner, C., Nickol, A., Seeba, J., Reuber, S., Junker, N., Wolter, M., Schneider, M. and Michaelis, A., "Understanding thickness and porosity effects on the electrochemical performance of $LiNi_{0.6}Co_{0.2}Mn_{0.2}O_2$-based cathodes for high energy Li-ion batteries," Journal of Power Sources 419, 119–126 (2019).